PI and Sliding Mode Control of a Multi-Input-Multi-Output Boost-Boost Converter

Zengshi Chen
GE Oil & Gas
811 Oak Willow Drive, Missouri City, Texas 77459, USA
chenzengshi@gmail.com

Weiwei Yong
Guangdong Medical College
Dongguan, Guangdong 523808, China

Wenzhong Gao
Department of Electrical and Computer Engineering
University of Denver, Denver, CO, USA

Abstract: - A proportional-integral (PI) controller and a sliding mode controller (SMC) are used to control a fourth-order Boost-Boost (BB) converter in continuous conduction mode with two input switches and two output voltages. Based on the equivalent control method, a closed-loop system is developed. The resultant PI gains have a nonlinear relationship with each other. The appropriate PI gains are obtained through the least squares method. The converter under the controller is stable and robust. The converter has voltage tracking accuracies within ±0.1 V for the first load and ±0.02 V for the second load. The maximum switching frequency is not greater than 100 KHz.

***Key-Words:* - PI, SMC, closed-loop, Boost-Boost, equivalent control method**

1 Introduction

The boost converter is a typical power component capable of amplifying the input voltage [1]. Two boost converters connected in tandem form a multi-variable DC-to-DC BB power converter [2]. Its two control switches are independently controlled. The application of a BB converter can be found in the situation in which one has to control the two loads independently under a single converter device. BB converters are able to step up a DC power supply through two loads. Based on the Generalized Proportional Integral (GPI) approach, a sliding mode feedback controller is developed for the regulation task [3]. A fully integrated single-inductor dual-output BB DC-DC converter with power-distributive control is designed [4]. This converter has better noise immunity, uses fewer power switches/external compensation components to reduce cost, and is thus suitable for system on chip applications. A controller for a quadratic boost converter with a single active switch is developed [5]. The average current-mode control methodology for an n-stage cascade boost converter is studied [6].

The great efforts have been made to improve dynamic response, transients and voltage ripples for DC-DC converters. It is claimed that boundary control can improve fast dynamic response [7]. The transients caused by the discontinuity in transition between buck and boost modes can be reduced by compensating the discontinuity and nonlinearity [8]. The energy transfer modes and output voltage ripple of a boost converter are analyzed within the given range of the input voltage and load with the emphasis of compact boost converters and intrinsically safe switching power supplies [9].

Various control methods have been developed for boost converters. The small signal based pulsewidth modulation (PWM) controllers are often used to regulate operating points locally [10-13]. Nonlinear controls for DC-DC converters have gained attention [2, 7, 14, 15]. They include but are not limited to flatness, passivity based control, dynamic feedback control by input-output

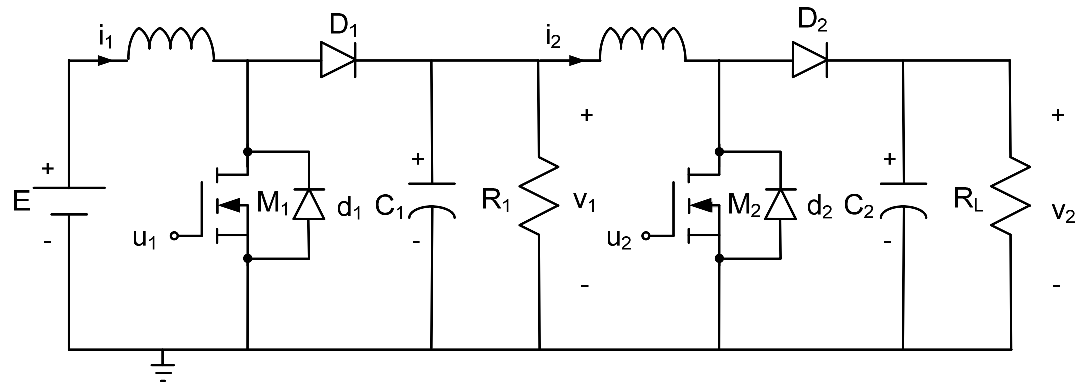

Fig. 1. Boost-Boost converter.

linearization, exact tracking, error passivity feedback, boundary control, and hybrid and optimal controls. Hysteresis control has been used for converters or inverters. A hysteretic current-mode control is applied to a buck converter with low voltage microprocessor loads [16]. A self-adjusting analog prediction of the hysteresis band is added to the phase-locked-loop control to ensure constant switching frequency of three-phase voltage-source inverters [17]. Hysteresis and delta modulation control is implemented for a buck converter by using sensorless current mode [18].

As a popular control method for converters and inverters, SMC has several merits, namely, large signal stability, robustness, good dynamic response, system order reduction and simple implementation [19]. SMC can be naturally implemented in converter control, since two discrete switching values can directly act as gating signals to semiconductor switching devices in power circuits [20]. The SMC generates more consistent transient responses for a wide operating range as compared with the conventional linear controls [21]. Open loop SMC is applied to various DC-DC converters. The indirect control of the current on a switching manifold is used for output voltage regulation. Open loop SMC lacks robustness against system uncertainties and disturbances [2, 22]. A PWM-Based sliding mode voltage controller is designed for basic DC-DC converters in continuous conduction mode [23]. Sliding mode controllers with dynamic sliding manifolds allow direct control of the voltages of buck, boost and buck-boost converters [24, 25]. SMC is applied to a buck converter with an assumption of the zero value of the average capacitor current [26]. A SMC analog integrated circuit for switching DC-DC converters is developed [27]. A small-signal model of boost converters with sliding mode control allows evaluation of closed-loop performances like audio-susceptibility, output and input impedances and reference to output transfer function [19].

PID control has been widely applied to industrial converters or inverters. Providing reliable PID tuning principles and finding appropriate PID gains are welcome by engineers and corporations [28]. The semi-global asymptotic stabilizing properties of classic PI control in the indirect regulation of average models of DC-DC converters are established [29]. A PID auxiliary dynamics is designed for a buck converter under SMC [30]. Generalized PI controllers are applied to buck, boost and buck-boost converters based on integral reconstructors of the unmeasured observable state variables [31]. A double-integral term of the controlled variables are added to alleviate the regulation in error of the DC-DC converter [32]. The phase portrait and the frequency design method are applied to a boost converter under the control of PI and SMC, the detailed analyses are provided for transient dynamics and non-minimum phase phenomena, and it is concluded that the non-minimum phase behavior always appears for a boost converter under such a controller [33].

This paper shows that PI and SMC control is applicable to a BB converter with two input switches and two output voltages. Through solving a highly nonlinear PI gain equation after the pole-placement, the approximate PI gains can be obtained. This paper is organized as follows. The BB converter model is developed in Section 2. The controller is designed and the closed-loop system is analyzed in Section 3. Simulation and results are reported in Section 4. Conclusion is in Section 5. References follow.

2 Boost-boost Converter Model

A BB converter that consists of two boost converters connected in tandem is shown in Fig. 1. It consists of an input voltage source E, two

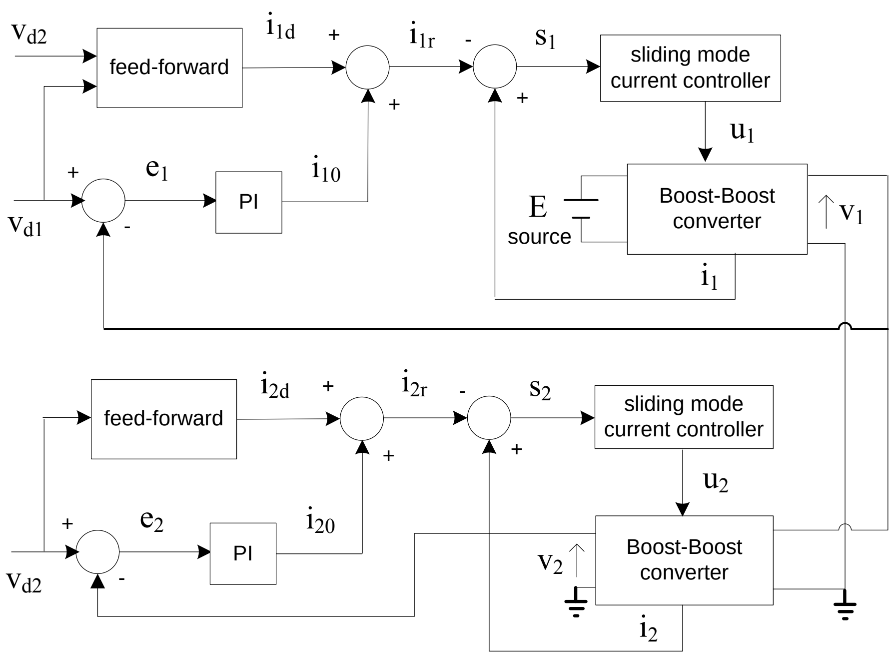

Fig. 2. PI and sliding mode control for Boost-Boost converter.

MOSFET switches M_1 and M_2, two anti-parallel diodes d_1 and d_2, two freewheeling diodes D_1 and D_2, two capacitors C_1 and C_2, two inductors L_1 and L_2, two load resistors R_1 and R_L. Let v_1 and v_2 be the voltages across C_1 and C_2, respectively. Let i_1 and i_2 be the currents through L_1 and L_2, respectively. u_1 and u_1 are sliding mode control signals applied at the gates of M_1 and M_2. M_1 and M_2 are independently controlled. As shown in [2], the ordinary differential equations for the BB converter are

$$i_1^{'} = -\frac{(1-u_1)}{L_1}v_1 + \frac{E}{L_1} \tag{1}$$

$$v_1^{'} = \frac{(1-u_1)}{C_1}i_1 - \frac{1}{C_1R_1}v_1 - \frac{1}{C_1}i_2 \tag{2}$$

$$i_2^{'} = \frac{1}{L_2}v_1 - \frac{1-u_2}{L_2}v_2 \tag{3}$$

$$v_2^{'} = \frac{(1-u_2)}{C_2}i_2 - \frac{1}{C_2R_L}v_2 \tag{4}$$

where ' means the first derivative. Eqs. 1, 2, 3 and 4 represent a typical variable structure system with the discontinuous right hand side. A bilinear relation exists between the control and the state variables.

3 Controller Design

3.1 Equilibrium points

The equilibrium points of the BB converter corresponding to constant values of the average control inputs are obtained by letting the right hand side of Eqs. 1, 2, 3 and 4 be zero while the control variables are set to be $u_1=U_1$ and $u_2=U_2$ where U_1 and U_2 are constants [2]. Let i_{1d}, v_{1d}, i_{2d}, and v_{2d} be the equilibrium points of i_1, v_1, i_2, and v_2, respectively. Eqs. 1, 2, 3 and 4 become

$$-(1-U_1)v_{1d} + E = 0 \tag{5}$$

$$(1-U_1)i_{1d} - \frac{1}{R_1}v_{1d} - i_{2d} = 0 \tag{6}$$

$$v_{1d} - (1-U_{2d})v_{2d} = 0 \tag{7}$$

$$(1-U_{2d})i_{2d} - \frac{1}{R_L}v_{2d} = 0 \tag{8}$$

Solving Eqs. (5), (6), (7) and (8) for i_{1d}, U_{1d}, i_{2d}, and U_{2d} in terms of the known v_{1d} and v_{2d} renders

$$\begin{aligned}&(i_{1d}, v_{1d}, i_{2d}, v_{2d}, U_1, U_2)\\ &= \Big(\frac{R_L v_{1d}^2 + R_1 v_{2d}^2}{ER_1R_L}, v_{1d}, \frac{v_{2d}^2}{R_L v_{Ld}},\\ &v_{2d}, \frac{v_{1d}-E}{v_{1d}}, \frac{v_{2d}-v_{1d}}{v_{2d}}\Big)\end{aligned} \tag{9}$$

Eq. 9 provides i_{1d}, i_{2d}, U_1 and U_2 as the functions of v_{1d} and v_{2d} in the steady state.

3.2 Closed-loop control

The control goal is to track two constant voltages v_{d1} and v_{d2}. The control structure for the converter is shown in Fig. 2 where i_{10} and i_{20} are the feedback reference currents, v_{1d} and v_{2d} are the reference voltages, E, v_1, v_2, i_1, i_2, u_1, and u_2 are defined previously, $e_1=v_{1d}-v_1$ and $e_2=v_{2d}-v_2$ are the voltage errors, and i_1 and i_2 are the positive feedback signals due to the structure of the sliding mode controllers as shown in Eqs. 16 and 17. The sensed information is needed for i_1, i_2, v_1 and v_2.

3.2.1 Voltage loop

A PI voltage controller can eliminate the voltage error caused by disturbance or uncertainty. The feedback reference currents generated by the BB converter are

$$i_{10} = K_{p1}e_1 + K_{i1}\int_0^t e_1 dt \tag{10}$$

$$i_{20} = K_{p2}e_2 + K_{i2}\int_0^t e_2 dt \tag{11}$$

where K_{p1} and K_{i1} are the proportional and integral gains for the first boost converter, respectively, and K_{p2} and K_{i2} are the proportional and integral gains for the second boost converter, respectively. Differentiating Eqs. 10 and 11 renders

$$i_{10}^{'} = K_{p1}e_1^{'} + K_{i1}e_1 \tag{12}$$

$$i_{20}^{'} = K_{p2}e_2^{'} + K_{i2}e_2 \tag{13}$$

Differentiating Eqs. 12 and 13 renders

$$i_{10}^{''} = K_{p1}e_1^{''} + K_{i1}e_1^{'} \tag{14}$$

$$i_{20}^{''} = K_{p2}e_2^{''} + K_{i2}e_2^{'} \tag{15}$$

The overall reference currents for the current loops of the BB converter are

$$i_{1r} = i_{1d} + i_{10} \tag{16}$$

$$i_{2r} = i_{2d} + i_{20} \tag{17}$$

where as shown in Eq. 9, i_{1d} and i_{2d}, the feedforward currents are $i_{1d} = \frac{R_L v_{1d}^2 + R_1 v_{2d}^2}{ER_1R_L}$ and $i_{2d} = \frac{v_{2d}^2}{R_L v_{Ld}}$. i_{1r} and i_{2r} are shown in Fig. 2.

3.2.2 Current loop

The switching manifolds for the sliding mode current controls are designed as

$$s_1 = i_1 - i_{1r} \tag{18}$$

$$s_2 = i_2 - i_{2r} \tag{19}$$

The control signals are

$$u_1 = 0.5(1 - sign(s_1)) = 1 \quad if\, s_1 < 0 \ or\ 0 \ if\, s_1 > 0 \tag{20}$$

$$u_2 = 0.5(1 - sign(s_2)) = 1 \quad if\, s_2 < 0 \ or\ 0 \ if\, s_2 > 0 \tag{21}$$

The existence condition of sliding mode can be derived with a candidate Lyapunov function [22]. Let this function be

$$P = 0.5s^Ts > 0 \quad \text{if } s \neq 0. \tag{22}$$

where $s = [s_1, s_2]^T$ where T is transpose. Differentiating Eq. 18 yields

$$\begin{aligned} s_1^{'} &= i_1^{'} - i_{10}^{'} = -\frac{(1-u_1)}{L_1}v_1 + \frac{E}{L_1} - i_{10}^{'} \\ &= -\frac{v_1}{2L_1}\operatorname{sgn}(s_1) + \frac{E}{L_1} - \frac{v_1}{2L_1} - i_{10}^{'} \end{aligned} \tag{23}$$

Differentiating Eq. 19 yields

$$\begin{aligned} s_2^{'} &= i_2^{'} - i_{20}^{'} = \frac{1}{L_2}v_1 - \frac{1-u_2}{L_2}v_2 - i_{20}^{'} \\ &= -\frac{v_2}{2L_2}\operatorname{sgn}(s_2) + \frac{v_1}{L_2} - \frac{v_2}{2L_2} - i_{20}^{'} \end{aligned} \tag{24}$$

With Eq. 22, the derivative of P is

$$\begin{aligned} P' &= ss' = s_1s_1^{'} + s_2s_2^{'} \\ &= s_1[-\frac{v_1}{2L_1}\operatorname{sgn}(s_1) + \frac{E}{L_1} - \frac{v_1}{2L_1} - i_{10}^{'}] \\ &+ s_2[-\frac{v_2}{2L_2}\operatorname{sgn}(s_2) + \frac{v_1}{L_2} - \frac{v_2}{2L_2} - i_{20}^{'}] \\ &= -\frac{v_1}{2L_1}|s_1| + (\frac{E}{L_1} - \frac{v_1}{2L_1} - i_{10}^{'})s_1 - \frac{v_2}{2L_2}|s_2| \\ &+ (\frac{v_1}{L_2} - \frac{v_2}{2L_2} - i_{20}^{'})s_2 \\ &\leq -\frac{v_1}{2L_1}|s_1| + |\frac{E}{L_1} - \frac{v_1}{2L_1} - i_{10}^{'}||s_1| \\ &- \frac{v_2}{2L_2}|s_2| + |\frac{v_1}{L_2} - \frac{v_2}{2L_2} - i_{20}^{'}||s_2| \\ &= |s_1|(|\frac{E}{L_1} - \frac{v_1}{2L_1} - i_{10}^{'}| - \frac{v_1}{2L_1}) \\ &+ |s_2|(|\frac{v_1}{L_2} - \frac{v_2}{2L_2} - i_{20}^{'}| - \frac{v_2}{2L_2}). \end{aligned} \tag{25}$$

A sufficient condition for $P' < 0$ is

$$|\frac{E}{L_1} - \frac{v_1}{2L_1} - i_{10}^{'}| - \frac{v_1}{2L_1} < 0 \tag{26}$$

$$|\frac{v_1}{L_2} - \frac{v_2}{2L_2} - i_{20}^{'}| - \frac{v_2}{2L_2} < 0 \tag{27}$$

Solving the inequalities (26) and (27) leads to

$$0 < E - L_1 i_{10}^{'} < v_1 \tag{28}$$

$$0 < v_1 - L_2 i_{20}^{'} < v_2 \tag{29}$$

In the steady state, $i_{10}^{'}$ and $i_{20}^{'}$ are equal to 0 due to constant i_{10} and i_{20}. The inequalities (28) and (29) degrade to be

$$0 < E < v_1 \tag{30}$$

$$0 < v_1 < v_2 \tag{31}$$

The above derivation shows $P' < 0$ if $E < v_1$ and $v_1 < v_2$. The inequalities (30) and (31) are satisfied by selecting $E<v_{d1}<v_{d2}$. Because the controls in Eqs. 20 and 21 contain no control gains to be adjusted, the domain of attraction (the inequalities (30) and (31)) are predetermined by the system architecture $E<v_{d1}<v_{d2}$. The derivation of Eq. 25 implicitly validates Eqs. 20 and 21 since it results in a stable system.

3.2.3 Closed-loop analysis

One can use the equivalent control method to analyze a discontinuous system [22]. Once the system is in sliding mode, s=0 and s'=0 are true. The continuous equivalent controls u_{1e} and u_{2e} replace the discontinuous controls u_1 and u_2 in s'=0. s'=0 is solved for u_{1e} and u_{2e}. After sliding mode occurs, one has $i_1= i_{10}$ and $i_2= i_{20}$. The derivatives of s are

$$s_1^{'} = i_1' - i_{10}'' = -\frac{(1-u_{1e})}{L_1} v_1 + \frac{E}{L_1} - i_{10}^{'} = 0 \tag{32}$$

$$s_2^{'} = i_2' - i_{20}' = \frac{1}{L_2} v_1 - \frac{1-u_{2e}}{L_2} v_2 - i_{20}^{'} = 0 \tag{33}$$

Solving Eq. 32 for u_{1e} renders

$$u_{1e} = \frac{v_1 - E + L_1 i_{10}^{'}}{v_1} \tag{34}$$

Solving Eq. 33 for u_{2e} renders

$$u_{2e} = \frac{v_2 - v_1 + L_2 i_{20}^{'}}{v_2} \tag{35}$$

Solving Eqs. 2 and 4 renders

$$i_{10} = \frac{C_1 v_1^{'} + \frac{v_1}{R_1} + \frac{C_2 v_2^{'} + \frac{v_2}{R_L}}{1-u_{2e}}}{1-u_{1e}} \tag{36}$$

$$i_{20} = \frac{C_2 v_2^{'} + \frac{v_2}{R_L}}{1-u_{2e}} \tag{37}$$

With Eqs. 11 and 37, one has

$$K_{p2}(v_{d2} - v_2) + K_{i2}\int_0^t (v_{d2} - v_2)dt = \frac{C_2 v_2^{'} + \frac{v_2}{R_L}}{1-u_{2e}} \tag{38}$$

Differentiating Eq. 35 renders

$$u_{2e}^{'} = \frac{(v_2^{'} - v_1^{'} + L_2 i_{20}^{''})v_2 - (v_1 - E + L_1 i_{10}^{'})v_2^{'}}{v_2^2} \tag{39}$$

Differentiating Eq. 38 renders

$$-K_{p2}v_2^{'} + K_{i2}(v_{d2} - v_2) = \frac{(C_2 v_2^{''} + \frac{v_2^{'}}{R_L})(1-u_{2e}) + (C_2 v_2^{'} + \frac{v_2}{R_L})u_{2e}^{'}}{(1-u_{2e})^2} \tag{40}$$

Plugging u_{2e}, $u_{2e}^{'}$, i_{10}, $i_{10}^{'}$, $i_{10}^{''}$, i_{20}, $i_{20}^{'}$ and $i_{20}^{''}$ into Eq. 40 renders

$$\begin{aligned}
&\{1 - \frac{v_2 - v_1 + L_2[-K_{p2}v_2^{'} + K_{i2}(v_{d2} - v_2)]}{v_2}\}^2 * \\
&[-K_{p2}v_2^{'} + K_{i2}(v_{d2} - v_2)] = \\
&(C_2 v_2^{''} + \frac{v_2^{'}}{R_L}) * \\
&\{1 - \frac{v_2 - v_1 + L_2[-K_{p2}v_2^{'} + K_{i2}(v_{d2} - v_2)]}{v_2}\} + \\
&(C_2 v_2^{'} + \frac{v_2}{R_L})\{\frac{[v_2^{'} - v_1^{'} - L_2(K_{p2}v_2^{''} + K_{i2}v_2^{'})]v_2}{v_2^2} \\
&- \frac{[v_2 - v_1 + L_2(-K_{p2}v_2^{'} + K_{i2}(v_{d2} - v_2))]}{v_2^2}\}v_2^{'}
\end{aligned}$$

(41)

Multiplying both sides of Eq. 41 by v_2^2 renders

$$\{v_1 + L_2(K_{p2}v_2^{'} - K_{i2}(v_{d2} - v_2))]\}^2 *$$
$$[-K_{p2}v_2^{'} + K_{i2}(v_{d2} - v_2)] =$$
$$v_2(C_2 v_2^{''} + \frac{v_2^{'}}{R_L})[v_1 + L_2[K_{p2}v_2^{'} - K_{i2}(v_{d2} - v_2)]$$
$$+(C_2 v_2^{'} + \frac{v_2}{R_L})\{[v_2^{'} - v_1^{'} - L_2(K_{p2}v_2^{''} + K_{i2}v_2^{'})]v_2$$
$$-[v_2 - v_1 + L_2[-K_{p2}v_2^{'} + K_{i2}(v_{d2} - v_2)]v_2^{'}\}.$$
(42)

Eq. 42 is a highly nonlinear equation in terms of v_1, v_2 and their derivatives of different orders. Linearizing Eq. 42 with respect to v_1, v_2 and their derivatives of different orders around their equilibrium points and carrying on a controller design are a practical approach. Let $v_{1\delta}$ and $v_{2\delta}$ be the perturbations of v_1 and v_2. One has $v_1 = v_{1\delta} + v_{d1}$, $v_2 = v_{2\delta} + v_{d2}$, $v_1^{'} = v_{1\delta}^{'}$, $v_2^{'} = v_{2\delta}^{'}$, $v_1^{''} = v_{1\delta}^{''}$, $v_2^{''} = v_{2\delta}^{''}$, $v_1^{'''} = v_{1\delta}^{'''}$, and $v_2^{'''} = v_{2\delta}^{'''}$. Plugging them into Eq. 42, dropping any term with the power of $v_{1\delta}$, $v_{2\delta}$, $v_{1\delta}^{'}$, $v_{2\delta}^{'}$, $v_{1\delta}^{''}$, $v_{2\delta}^{''}$, $v_{1\delta}^{'''}$, and $v_{2\delta}^{'''}$ greater than 1, and dropping any product of some of them and any of these variables with a higher power render a linear ordinary differential equation as

$$P_3 v_{2\delta}^{''} + P_2 v_{2\delta}^{'} + P_1 v_{2\delta} = v_{1\delta}^{'} \quad (43)$$

where $P_1 = P_{11}K_{i2} = -\frac{R_L v_{10}^2}{v_{20}^2}K_{i2}$,

$$P_2 = P_{21}K_{p2} + P_{22}K_{i2} + P_{23}$$
$$= -\frac{R_L v_{10}^2}{v_{20}^2}K_{p2} + L_2 K_{i2} - \frac{v_{10}v_{20} + v_{20}^2 - v_{20}(v_{20} - v_{10})}{v_{20}^2}$$

and $P_3 = P_{31}K_{p2} + P_{32} = -L_2 K_{p2} + \frac{v_{10}R_L C_2}{v_{20}}$. With Eqs. 10 and 36, one has

$$K_{p1}(v_{d1} - v_1) + K_{i1}\int_0^t (v_{d1} - v_1)dt$$
$$= \frac{C_1 v_1^{'} + \frac{v_1}{R_1} + \frac{C_2 v_2^{'} + \frac{v_2}{R_L}}{1 - u_{2e}}}{1 - u_{1e}} \quad (44)$$

Differentiating Eq. 44 renders

$$-K_{p1}v_1^{'} + K_{i1}(v_{d1} - v_1) =$$
$$\frac{(C_1 v_1^{''} + \frac{v_1^{'}}{R_1})(1 - u_{1e}) + (C_1 v_1^{''} + \frac{v_1^{'}}{R_1})u_{1e}^{'}}{(1 - u_{1e})^2} + \quad (45)$$
$$\frac{(C_2 v_2^{''} + \frac{v_2^{'}}{R_L})(1 - u_{1e})(1 - u_{2e}) - (C_2 v_2^{'} + \frac{v_2}{R_1})(-u_{1e}^{'} - u_{2e}^{'} + u_{1e}^{'}u_{2e} + u_{1e}u_{2e}^{'})}{(1 - u_{1e})^2(1 - u_{2e})^2}$$

Rearranging Eq. 45 renders

$$(-K_{p1}v_1^{'} + K_{i1}(v_{d1} - v_1))(1 - u_{1e})^2(1 - u_{2e})^2 =$$
$$[(C_1 v_1^{''} + \frac{v_1^{'}}{R_1})(1 - u_{1e}) + (C_1 v_1^{''} + \frac{v_1^{'}}{R_1})u_{1e}^{'}](1 - u_{2e})^2 +$$
$$(C_2 v_2^{''} + \frac{v_2^{'}}{R_L})(1 - u_{1e})(1 - u_{2e}) - (C_2 v_2^{'} + \frac{v_2}{R_1}) *$$
$$(-u_{1e}^{'} - u_{2e}^{'} + u_{1e}^{'}u_{2e} + u_{1e}u_{2e}^{'})$$
(46)

Plugging u_{1e}, u_{2e}, $u_{1e}^{'}$, $u_{2e}^{'}$, $i_{10}^{'}$, $i_{10}^{''}$, $i_{20}^{'}$ and $i_{20}^{''}$ into Eq. 46 and expanding it render

$$[-K_{p1}v_1^{'} + K_{i1}(v_{d1} - v_1)][E + L_1 K_{p1}v_1^{'} -$$
$$L_1 K_{i1}(v_{d1} - v_1)]^2[v_1 + L_2 K_{p2}v_2^{'} - L_2 K_{i2}(v_{d2} - v_2)]^2$$
$$= v_1(C_1 v_1^{''} + \frac{v_1^{'}}{R_1})[E + L_1 K_{p1}v_1^{'} - L_1 K_{i1}(v_{d1} - v_1)][v_1$$
$$+ L_2 K_{p2}v_2^{'} - L_2 K_{i2}(v_{d2} - v_2)]^2 - (C_1 v_1^{'} + \frac{v_1}{R_1})[-Ev_1^{'}$$
$$+ L_1 K_{p1}v_1 v_1^{''} + L_1 K_{i1}v_1 v_1^{'} - L_1 K_{p1}v_1^{'}v_1^{'}$$
$$+ L_1 K_{i1}v_1^{'}(v_{d1} - v_1)][v_1 + L_2 K_{p2}v_2^{'}$$
$$- L_2 K_{i2}(v_{d2} - v_2)]^2 + v_1 v_2(C_2 v_2^{''} + \frac{v_2^{'}}{R_L})[E +$$
$$L_1 K_{p1}v_1^{''} - L_1 K_{i1}(v_{d1} - v_1)][v_1$$
$$+ L_2 K_{p2}v_2^{'} - L_2 K_{i2}(v_{d2} - v_2)] - (C_2 v_2^{'} +$$
$$\frac{v_2}{R_2})\{v_2^2 v_1 L_1 K_{p1}v_1^{''} + v_2^2 v_1 L_1 K_{i1}v_1^{'} + v_2^2 v_1^{'}[-E$$
$$- L_1 K_{p1}v_1^{'} + L_1 K_{i1}(v_{d1} - v_1)] - [v_2(-v_1^{'} -$$
$$L_2 K_{p2}v_2^{''} - L_2 K_{i2}v_2^{'}) - v_2^{'}(-v_1 - L_2 K_{p2}v_2^{'}$$
$$+ L_2 K_{i2}(v_{d2} - v_2))]v_1^2 + v_2[-v_1 L_1 K_{p1}v_1^{''} - v_1 L_1 K_{i1}v_1^{'} -$$

$$v_1'(-E + L_1K_{p1}v_1' - v_1L_1K_{i1}(v_{d1} - v_1))](v_2 - v_1 - L_2K_{p2}v_2' + L_2K_{i2}(v_{d2} - v_2)) + v_1[v_1 - E - L_1K_{p1}v_1' + L_1K_{i1}(v_{d1} - v_1)][-v_2v_1' - v_2L_2K_{p2}v_2'' - v_2L_2K_{i2}v_2' + v_1v_2' + L_2K_{p2}v_2'v_2' - L_2K_{i2}(v_{d2} - v_2)v_2']\} - v_1L_1K_{p1}v_1'' - v_1L_1K_{i1}v_1' - v_1'(-E + L_1K_{p1}v_1' - v_1L_1K_{i1}(v_{d1} - v_1))](v_2 - v_1 - L_2K_{p2}v_2' + L_2K_{i2}(v_{d2} - v_2))$$

(47)

Eq. 47 is a highly nonlinear equation in terms of v_1, v_2 and their derivatives of different orders. Linearizing Eq. 47 with respect to v_1, v_2 and their derivatives of different orders around their equilibrium points and carrying on a controller design are a practical approach. Let $v_{1\delta}$ and $v_{2\delta}$ be the perturbations of v_1 and v_2. One has $v_1 = v_{1\delta} + v_{d1}$, $v_2 = v_{2\delta} + v_{d2}$, $v_1' = v_{1\delta}'$, $v_2' = v_{2\delta}'$, $v_1'' = v_{1\delta}''$, $v_2'' = v_{2\delta}''$, $v_1''' = v_{1\delta}'''$, and $v_2''' = v_{2\delta}'''$. Plugging them into Eq. 47, dropping any term with the power of $v_{1\delta}$, $v_{2\delta}$, $v_{1\delta}'$, $v_{2\delta}'$, $v_{1\delta}''$, $v_{2\delta}''$, $v_{1\delta}'''$, and $v_{2\delta}'''$ greater than 1, and dropping any product of some of them and any of these variables with a higher power render a linear ordinary differential equation as

$$a_3v_{1\delta}'' + a_2v_{1\delta}' + a_1v_{1\delta} + b_3v_{2\delta}'' + b_2v_{2\delta}' = 0 \qquad (48)$$

where $a_1 = a_{11}K_{i1} = E^2v_{10}^2K_{i1}$,

$$a_2 = a_{21}K_{p1} + a_{22}K_{i1} + a_{23} = E^2v_{10}^2K_{p1} - \left(\frac{v_{10}^4L_1}{R_1} + \frac{v_{20}^3v_{10}L_1 - v_{20}^2(v_{20} - v_{10})v_{10}L_1}{R_L}\right)K_{i1} + \frac{2v_{10}^3E}{R_1} + \frac{v_{20}^3E - v_{10}^2v_{20}^2 - v_{20}^2(v_{20} - v_{10})E + v_{20}^2v_{10}(v_{10} - E)}{R_L},$$

$$a_3 = a_{31}K_{p1} + a_{32} = -\left[\frac{v_{10}^4L_1}{R_1} + \frac{v_{20}^3v_{10}L_1 - v_{20}^2v_{10}(v_{20} - v_{10})L_1}{R_L}\right]K_{p1}, + C_1v_{10}^3E$$

$$b_2 = b_{21}K_{i2} + b_{22} = \left[\frac{L_2v_{10}v_{20}^2(v_{10} - E) - L_2v_{10}^2v_{20}^2}{R_L}\right]K_{i2} + \frac{Ev_{10}^2v_{20} + v_{10}^3v_{20} - v_{10}^2v_{20}(v_{10} - E)}{R_L}$$

and

$$b_3 = b_{31}K_{p2} + b_{32} = \left[\frac{L_2v_{10}v_{20}^2(v_{10} - E) - L_2v_{10}^2v_{20}^2}{R_L}\right]K_{p2} + C_2Ev_{10}^2v_{20}$$

.

Differentiating Eq. 43 renders

$$P_3v_{2\delta}''' + P_2v_{2\delta}'' + P_1v_{2\delta}' = v_{1\delta}'' \qquad (49)$$

Differentiating Eq. 49 renders

$$P_3v_{2\delta}^{(4)} + P_2v_{2\delta}''' + P_1v_{2\delta}'' = v_{1\delta}''' \qquad (50)$$

Differentiating Eq. 48 renders

$$a_3v_{1\delta}''' + a_2v_{1\delta}'' + a_1v_{1\delta}' + b_3v_{2\delta}''' + b_2v_{2\delta}'' = 0 \qquad (51)$$

Substituting Eqs. 43, 49 and 50 into Eq. 51 renders

$$a_3P_3v_{2\delta}^{(4)} + (a_3P_2 + a_2P_3 + b_3)v_{2\delta}''' + (a_3P_1 + a_2P_2 + a_1P_3 + b_2)v_{2\delta}'' + (a_2P_1 + a_1P_2)v_{2\delta}' + a_1P_1v_{2\delta} = 0 \qquad (52)$$

The characteristic equation of Eq. 52 is

$$S^4 + \frac{a_3P_2 + a_2P_3 + b_3}{a_3P_3}S^3 + \frac{a_3P_1 + a_2P_2 + a_1P_3 + b_2}{a_3P_3}S^2 + \frac{a_2P_1 + a_1P}{a_3P_3}S + \frac{a_1P_1}{a_3P_3} = 0 \qquad (53)$$

Assuming Eq. 53 has four equal and negative poles, one has the desired closed-loop system characteristic equation as

$$(S - S_0)(S - S_0)(S - S_0)(S - S_0) = 0 \qquad (54)$$

Expanding Eq. 54 renders

$$S^4 - 4S_0S^3 + 6S_0^2S^2 + 4S_0^3S + S_0^4 = 0 \qquad (55)$$

Making Eq. 53 and Eq. 55 equal to each other, one has

$$a_3P_2 + a_2P_3 + b_3 = -4S_0a_3P_3 = aa_3P_3 \qquad (56)$$

$$a_3P_1 + a_2P_2 + a_1P_3 + b_2 = 6S_0^2a_3P_3 = ba_3P_3 \qquad (57)$$

$$a_2P_1 + a_1P_2 = 4S_0^3a_3P_3 = ca_3P_3 \qquad (58)$$

$$a_1P_1 = S_0^4a_3P_3 = da_3P_3 \qquad (59)$$

With Eq. 59, one has

$$a_3P_3 = \frac{a_1P_1}{d} \qquad (60)$$

Plugging Eq. 60 into Eqs. 56, 57 and 58 renders

$$a_3P_2 + a_2P_3 + b_3 = \frac{a}{d}a_1P_1 \quad (61)$$

$$a_3P_1 + a_2P_2 + a_1P_3 + b_2 = \frac{b}{d}a_1P_1 \quad (62)$$

$$a_2P_1 + a_1P_2 = \frac{c}{d}a_1P_1 \quad (63)$$

Next, the nonlinear equations for K_{p1}, K_{p2}, K_{i1}, and K_{i2} are obtained by solving Eqs. 59, 61, 62 and 63. Rearranging Eq. 61 renders

$$q_{11}K_{p1}K_{p2} + q_{12}K_{p1}K_{i2} + q_{13}K_{i1}K_{p2} + q_{14}K_{i1}K_{i2} + q_{15}K_{p1} + q_{16}K_{p2} + q_{17}K_{i1} + q_{18}K_{i2} + q_{19} = 0. \quad (64)$$

where $q_{11} = a_{21}P_{32} + a_{31}P_{21}$, $q_{12} = a_{31}P_{22}$, $q_{13} = a_{22}P_{31}$, $q_{14} = -\frac{a}{d}a_{11}P_{11}$, $q_{15} = a_{31}P_{23} + a_{21}P_{32}$, $q_{16} = a_{32}P_{21} + a_{23}P_{31} + b_{31}$, $q_{17} = P_{32}a_{22}$, $q_{18} = a_{32}P_{22}$, and $q_{19} = a_{32}P_{23} + a_{23}P_{32} + b_{32}$.

Rearranging Eq. 62 renders

$$q_{21}K_{p1}K_{p2} + q_{22}K_{p1}K_{i2} + q_{23}K_{i1}K_{p2} + q_{24}K_{i1}K_{i2} + q_{25}K_{p1} + q_{26}K_{p2} + q_{27}K_{i1} + q_{28}K_{i2} + q_{29} = 0. \quad (65)$$

where $q_{21} = a_{21}P_{21}$, $q_{22} = a_{31}P_{11} + a_{21}P_{22}$, $q_{23} = a_{22}P_{21} + a_{11}P_{31}$, $q_{24} = a_{22}P_{22} - \frac{b}{d}a_{11}P_{11}$, $q_{25} = a_{21}P_{23}$, $q_{26} = a_{23}P_{21}$, $q_{27} = a_{22}P_{23} + a_{11}P_{32}$, $q_{28} = a_{32}P_{11} + a_{23}P_{22} + b_{21}$, and $q_{29} = a_{23}P_{23} + b_{22}$.

Rearranging Eq. 63 renders

$$q_{31}K_{p1}K_{i2} + q_{32}K_{i1}K_{p2} + q_{33}K_{i1}K_{i2} + q_{34}K_{i1} + q_{35}K_{i2} = 0 \quad (66)$$

where $q_{31} = a_{21}P_{11}$, $q_{32} = a_{11}P_{21}$, $q_{33} = a_{11}P_{22} + (a_{22} - \frac{c}{d}a_{11})P_{11}$, $q_{34} = a_{11}P_{23}$, and $q_{35} = a_{23}P_{11}$.

Rearranging Eq. 59 renders

$$q_{41}K_{p1}K_{p2} + q_{42}K_{i1}K_{i2} + q_{43}K_{p1} + q_{44}K_{p2} + q_{45} = 0 \quad (67)$$

where $q_{41} = da_{31}P_{31}$, $q_{42} = -a_{11}P_{11}$, $q_{43} = da_{31}P_{32}$, $q_{34} = da_{32}P_{31}$, and $q_{45} = da_{32}P_{32}$.

Grouping Eqs. 64, 65, 66 and 67 renders a matrix equation as

$$AK_{pi} = B \quad (68)$$

where

$$A = \begin{bmatrix} q_{11} & q_{12} & q_{13} & q_{14} & q_{15} & q_{16} & q_{17} & q_{18} \\ q_{21} & q_{22} & q_{23} & q_{24} & q_{25} & q_{26} & q_{27} & q_{28} \\ 0 & q_{31} & q_{32} & q_{33} & 0 & 0 & q_{34} & q_{35} \\ q_{41} & 0 & 0 & q_{42} & q_{43} & q_{44} & 0 & 0 \end{bmatrix},$$

$$K_{pi} = \begin{bmatrix} K_{p1}K_{p2} \\ K_{p1}K_{i2} \\ K_{i1}K_{p2} \\ K_{i1}K_{i2} \\ K_{p1} \\ K_{p2} \\ K_{i1} \\ K_{i2} \end{bmatrix} \text{ and } B = \begin{bmatrix} -q_{19} \\ -q_{29} \\ 0 \\ -q_{45} \end{bmatrix}.$$

Eqs. 64, 65, 66 and 67 are nonlinear and there may exist a solution. To satisfy the control purpose, it is good enough to find the neighborhood of a solution in which any value for K_{p1}, K_{p2}, K_{i1}, and K_{i2} will render a robust power converter. One may use a numerical method to find the approximate K_{p1}, K_{p2}, K_{i1}, and K_{i2}. For example, one may eliminate K_{p2}, K_{i1}, and K_{i2} from Eqs. 64, 65, 66 and 67, and obtain a highly nonlinear algebraic equation for K_{p1}. Then one numerically finds an approximate value for K_{p1}. The approximate values for K_{p2}, K_{i1}, and K_{i2} are then obtained. However, in this paper, the least square method is used for obtaining approximate K_{p1}, K_{p2}, K_{i1}, and K_{i2}. With the least square method, the solution for Eq. 68 is

$$K_{pi} = (A^T A)^{-1} A^T B \quad (69)$$

The last four elements in the column array K_{pi} act as approximate K_{p1}, K_{p2}, K_{i1}, and K_{i2}. Later on the simulation shows the validity of this method. If the two slow and dominant poles among the four poles of Eq. 52 are considered, the trajectories of a nonlinear system in a small neighborhood of an equilibrium point is expected to be close to the trajectories of its linearization about that point if the origin of the linearized state equation is a hyperbolic equilibrium point [34]. Approximate PI gains guarantee a hyperbolic equilibrium point.

Table 1: Nominal Parameters

parameter	value	parameter	value
E_0	12 V	K_{p1}	1.568×10^{-5}
R_{10}	52 Ω	K_{p2}	-9.081×10^{-5}
C_{10}	48 μF	K_{i1}	14.261
L_{10}	15.91 mH	K_{i2}	0.797
R_{L0}	52 Ω	v_{d1}	15 V
C_{20}	107 μF	v_{d2}	24 V
L_{20}	40 mH	f	100 KHz
S_0	-600		

4 Simulation and Results

4.1 Pole placement

If the poles are closer to zero, the system will have advantages for passing low frequency signals and rejecting noises, but the system response is slower. Moreover, disturbances or uncertainties can easily bring the system to instability. As the poles are far from zero, the system response is faster and the system stability is better but the output may have magnified noises. One should compromise noise suppression, stability and response speed for pole selection. The pole situation of Eq. 53 for a stable BB converter can be: a) four real and negative poles; b) two real and negative poles and a pair of complex conjugated poles with negative and real parts; c) two pairs of complex conjugated poles with negative and real parts. Let the four poles be equal to each other and negative. For example, as a compromise, the desired pole S_0 =-600 is used. The nominal parameters are listed in Table 1. The four PI gains are listed in Table 1. The PI gains are not limited to these values. The acceptable values of PI gains should be around the neighbourhood of these PI values. One can refine these PI gains to achieve a desired system response. Substituting the PI values and other nominal parameters in Table 1 to Eq. 53 renders

$$S^4 + 1775S^3 + 741538S^2 + 85073064S + 1108171577 = 0 \tag{70}$$

whose four poles are S_{01}=-1227, S_{02}=-370, S_{03}=-164, and S_{04}=-15. These are the actual poles for Eq. 53.

4.2 Validation circuit

A BB converter with the proposed controller is constructed with Simulink as shown in Fig. 3. The converter is operated in the continuous mode. To show the capability of the controller, the feedforward input currents i_{1d} and i_{2d} are disabled. To implement the controller, the requirement for the system performances shall be evaluated, the appropriate BB converter parameters shall be selected, the appropriate PI gains shall be generated and Eqs. 10, 11, 18, 19, 20 and 21 shall be coded.

4.3 Results

Some circuit parameters are perturbed from their nominal values. The actual values of the inductors and capacitors used in the validation circuit in Fig. 3 are L_1=1.5L_{10}=23.865 mH, L_2=1.5L_{20}=60 mH, C_1=1.5C_{10}=72 μF, and C_2=1.5C_{20}=160.5 μF. The system responses under the following conditions are reported: 1) the reference voltages are constant values as given in Table 1; 2) the reference voltages have multi-step changes; 3) the input voltage has a multi-step change; 4) the load resistance has a multi-step change. The undershoot, overshoot, or non-minimum phase of a transient of the output voltage is discussed. The fixed-step size of simulation is 10 ìs. Since this paper deals with only simulation without A/D converters, 10 ìs is also the sampling period. Hence, the minimum sliding mode pulse width is 10 ìs or the maximum sliding mode switching frequency is 100 KHz. If the switching frequency is too low (e.g., less than 1 KHz), the proposed controller will fail to function. A system on a wide pulse is almost under open-loop control and diverges. As the switching frequency increases, the pulse width decreases, and the results are more desirable. The initial conditions of $i_1(0)= i_2(0)=0$ A and $v_1(0)= v_2(0)=0$ V are used for all the simulations.

4.3.1 Reference voltages with Single step change

Eq. 53 has the four poles -431 ± 57i, -168 and -16. As shown in the windows of the mid row of Fig. 4, within 0.3 seconds, v_1 converges to 15 V within ± 0.1 V with an oscillation and v_2 converges to 24 V within ±0.02 V with an oscillation. Nevertheless, the transient of v_2 does not overshoot beyond its steady state value. v_2 goes in the opposite direction before it reaches its steady state value. There is a detailed explanation for this kind of non-minimum phase phenomenon in Section 4.5 of [33]. The reference voltages are well tracked with high accuracy. The system responses are fast. The windows of the top row show the convergent currents i_1 and i_2. The windows of the bottom row show the sliding control signals u_1 and u_2.

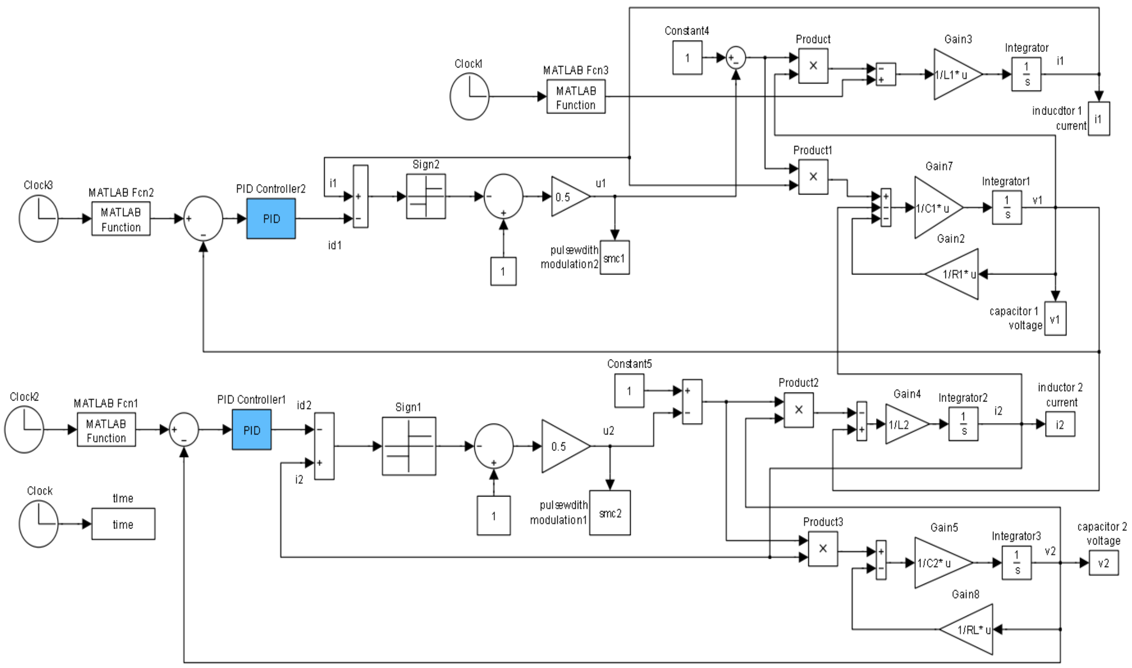

Fig. 3. Simulation circuit for the Boost-Boost converter.

4.3.2 Reference voltages with multi-step change

As shown in the windows of the mid row of Fig. 5, from the time point of 0 seconds to the time point of 0.5 seconds, v_1 and v_2 converge to v_{d1}=15 V and v_{d2}=24 V, respectively; from the time point of 0.5 seconds to the time point of 1.0 seconds, v_1 and v_2 converge to v_{d1}=20 V and v_{d2}=30 V, respectively; from the time point of 1.0 seconds to the time point of 1.5 seconds, v_1 and v_2 converge to v_{d1}=15 V and v_{d2}=24 V, respectively. The transients in the first 0.5 seconds are similar to the ones in Section IV.C.1. Starting at the time points of 0.5 seconds and 1.0 seconds, v_1 and v_2 go in the opposite directions before they converge to the steady state values. These non minimum phase behaviors are explained in detail in [33]. The tracking error bands for v_1 and v_2 are within ± 0.1 V and ±0.02 V, respectively. The reference voltages are well tracked accurately. The system response time after the first transient is about 0.15 seconds. The windows of the top row show the convergent currents i_1 and i_2. The windows of the bottom row show the sliding control signals u_1 and u_2.

4.3.3 Reference voltages with multi-step change

E is equal to 12 V in the first 0.5 seconds, 8 V in the second 0.5 seconds, and 12 V in the last 0.5 seconds. As shown in the windows of the mid row, v_1 and v_2 converge to v_{d1}=15 V and v_{d2}=24 V after each transient, respectively. As shown in the windows of the mid row of Fig. 6, at the time point of 0.5 seconds, since E steps down from 12 V to 8 V, v_1 and v_2 have the undershoots (goes less than 15 V and 24 V, respectively, and converge to 15 V and 24 V, respectively); At the time point of 1.0 seconds, since E steps up from 8 V to 12 V, v_1 and v_2 have the overshoots (goes greater than 15 V and 24 V, respectively, and converge to 15 V and 24 V, respectively). These transients cannot be explained by non-minimum or minimum phase. Instead, by perturbing E and v_1 or v_2 from their equilibrium points, one obtains the transfer function from E to v_1 or v_2. One can predict these transients by simulating and analyzing these transfer functions. The details are referred to [33]. The tracking error bands for v_1 and v_2 are within ± 0.1 V and ±0.02 V, respectively. The system response time after the first transient is about 0.15 seconds. The windows of the top row show the convergent currents i_1 and i_2. The windows of the bottom row show the sliding control signals u_1 and u_2.

4.3.4 Step change of load resistance

R_1 is equal to 52 Ω in the first 0.5 seconds, 42 Ω in the second 0.5 seconds, and 52 Ω in the last 0.5 seconds. R_L is equal to 52 Ω in the first 0.5 seconds, 62 Ω in the second 0.5 seconds, and 52 Ω in the last 0.5 seconds. As shown in the windows of the mid row of Fig. 7, v_1 and v_2 converge to v_{d1}=15 V and v_{d2}=24 V after each transient, respectively. At the time point of 0.5 seconds, since R_1 steps down from 52 V to 42 V, v_1 has the undershoot; since R_L steps up from 52 V to 62 V, v_2 has the overshoot. At the time point of 1.0 seconds, since R_1 steps up from 42 V to 52 V, v_1 has the overshoot; since R_L steps

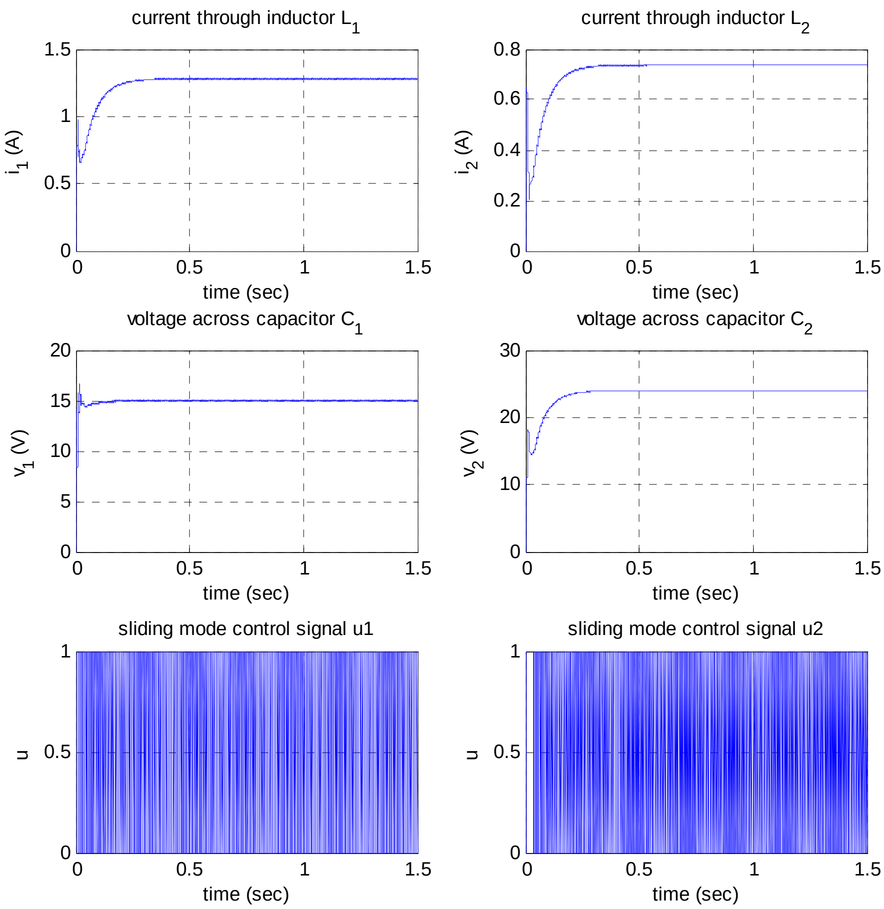

Fig. 4. The response of the Boost-Boost converter under reference voltages of single step change.

down from 62 V to 52 V, v_2 has the undershoot. These transients are not non-minimum phase. Instead, by perturbing R_l and v_1 or R_L and v_2 from their equilibrium points, one obtains the transfer function from R_l to v_1 or R_L to v_2. One can predict these transients by simulating and analyzing these transfer functions. The details are referred to [33]. The tracking error bands for v_1 and v_2 are within ± 0.1 V and ±0.02 V, respectively. The response time of v_1 after the first transient is about 0.05 seconds. The response time of v_2 after the first transient is about 0.25 seconds. The windows of the top row show the convergent currents i_1 and i_2. The windows of the bottom row show the sliding control signals u_1 and u_2.

5 Conclusion

This paper studies an analytical solution to a Boost-Boost converter with multi-inputs and multi-outputs under PI and sliding mode control. Via the equivalent control method, a fourth-order closed-loop nonlinear ordinary differential equation is obtained and linearized. Through the pole placement, a highly nonlinear equation for PI gains is obtained. The least square method or a numerical method is used to solve this nonlinear PI gain equation for approximate PI gains. The transients of the load voltages caused by step changes of various circuit parameters are predictable. With a validation circuit and large variation of inductances and capacitances, the simulation results show the controller has high tracking accuracy, strong system robustness and fast transient responses. The future work includes a study for the solutions that can result in a critically damped closed-loop system with a minimum phase, detailed analysis of all the transients, and an analytical solution of PI gains.

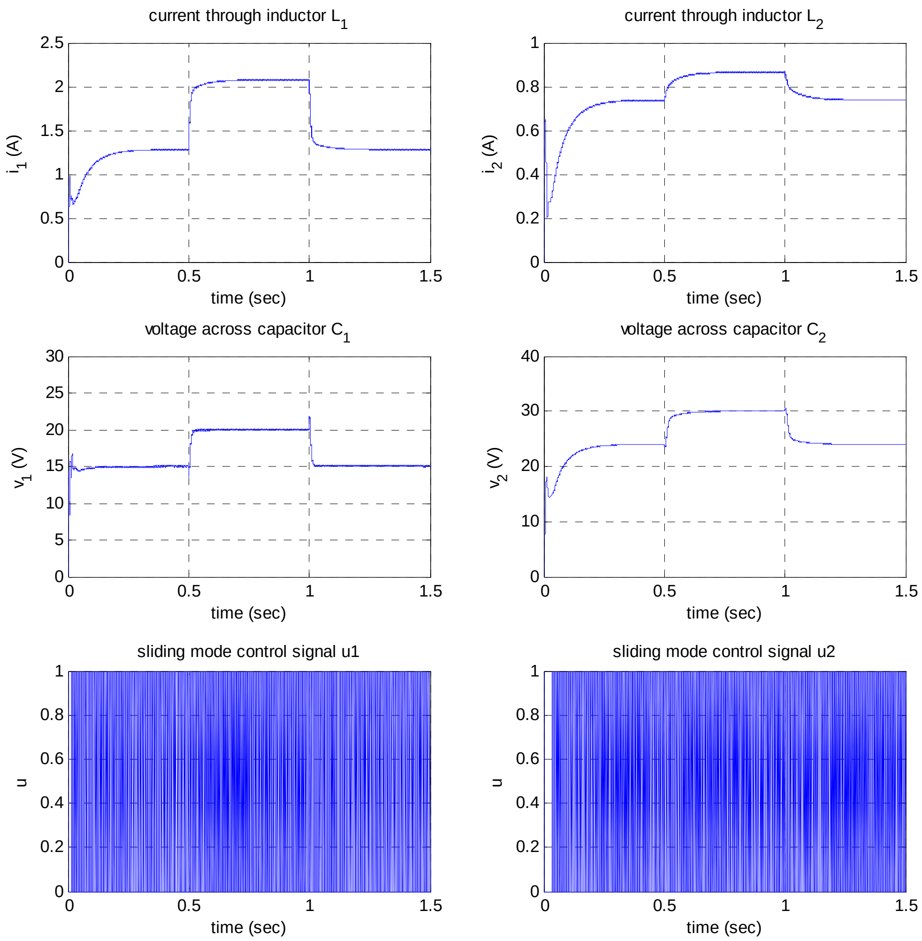

Fig. 5. The response of the Boost-Boost converter under reference voltages of multi-step change.

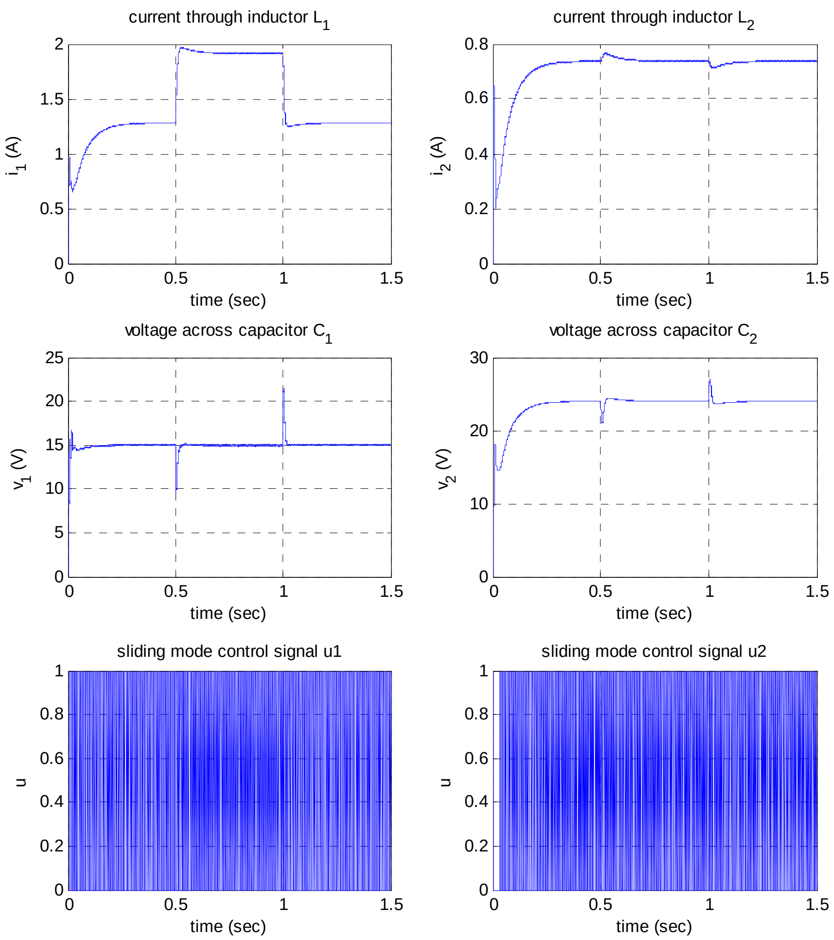

Fig. 6. The response of the Boost-Boost converter under input voltage of multi-step change.

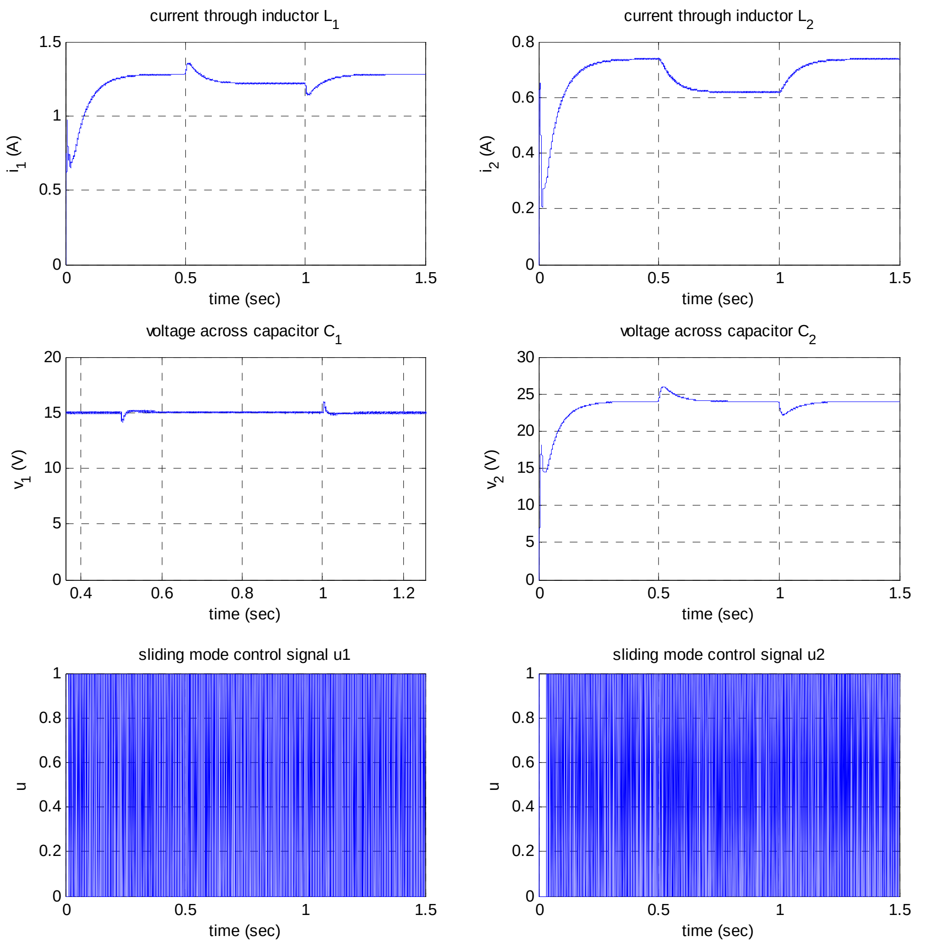

Fig. 7. The response of the Boost-Boost converter under load resistances of multi-step change.

References

[1] R. S. Weissbach, and K. M. Torres, "A Non-inverting buck-boost converter with reduced components using a microcontroller," *in Proc. IEEE Southeast Conference*, Aug. 2002, pp. 79-84.

[2] H. Sira-Ramirez and R. Silva-Origoza, *Control Design Techniques in Power Electronics Devices*. New Mexico City: Springer, 2006.

[3] A. Franco-Gonzalez, R. Marquez, and H. Sira-Ramirez, "On the Generalized-Proportional-Integral Sliding Mode Control of the "Boost Boost" Converter," in Proc. IEEE *4th Intl. Conf. on Electrical and Electronics Eng.*, 2007, Mexico City, Mexico.

[4] H. W. Chang, W. H. Chang, and C. H. Tsai, "Integrated single-inductor buck-boost or boost-boost DC-DC converter with power-distributive control," in *Proc. Intl. Conf. Power Electronics and Drive Systems*, Nov. 2009.

[5] J. Leyva-Ramos, M. G. Ortiz-Lopez, L. H. Díaz-Saldierna, and J. A. Morales-Saldaña, "Switching regulator using a quadratic boost converter for wide DC conversion ratios," *IET Power Electronics*, vol. 2, no. 5, pp. 605-613, 2009.

[6] J. Leyva-Ramos, M. G. Ortiz-Lopez, L. H. Díaz-Saldierna, and M. Martinez-Cruz, "Average current controlled switching regulators with cascade boost converters," *IET Power Electronics*, vol. 4, no. 1, pp. 1-10, 2011.

[7] T. T. Song, and H. S. Chung, "Boundary Control of Boost Converters Using State-Energy Plane," *IEEE Transactions on Power Electronics*, vol. 23, no. 2, pp. 551-563, Mar. 2008.

[8] Y. J. Lee, A. Khaligh, and A. Emadi, "A Compensation Technique for Smooth Transitions in a Non-inverting Buck–Boost Converter," *IEEE Transactions on Power Electronics*, vol. 24, no. 4, Apr. 2009.

[9] S. L. Liu, et al., "Analysis of Operating Modes and Output Voltage Ripple of Boost DC–DC Converters and Its Design Considerations," *IEEE Transactions on Power Electronics*, vol. 23, no. 4, pp. 1813-1821, Jul. 2008.

[10] R. W. Erickson, and D. Maksimovic, *Fundamentals of Power Electronics*. Boston, USA: Kluwer Academic Publishers, 2004.

[11] D. Xu, C. Zhao, and H. Fan, "A PWM Plus Phase Shift Control Bidirectional DC-DC Converter," *IEEE Transactions on Power Electronics*, vol. 19, no. 13, pp. 666-675, May. 2004.

[12] D. M. Mitchell, *DC-DC Switching Regulator Analysis*. New York: McGraw-Hill, 1998.

[13] A. J. Forsyth, and S. V. Mollow, "Modeling and Control of DC-DC Converters," *Power Engineering Journal*, vol. 12, no.5, pp. 229 -236, Aug. 1998.

[14] G. Chu, et al., "A Unified Approach for the Derivation of Robust Control for Boost PFC Converters," *IEEE Transactions on Power Electronics*, vol. 24, no. 1, pp. 2531-2544, Nov. 2009.

[15] S. Mariethoz, et al., "Comparison of Hybrid Control Techniques for Buck and Boost DC -DC Converters," *IEEE Transactions on Control Systems Technology*, Early Access, 2010.

[16] B. Arbetter and D. Maksimovic, "DC-DC converter with fast transient response and high efficiency for low-voltage microprocessor loads," *in Proc.IEEE Applied Power Electronics*, vol. 1, pp. 156-162, Feb. 1998.

[17] L. Malesani, P. Mattavelli, and P. Tomasin, "Improved constant-frequency hysteresis current control of VSI inverters with simple feedforward bandwidth prediction," *IEEE Transactions on Industry Applications*, vol. 33, no. 5, pp. 1194-1202, Sept./Oct. 1997.

[18] J. W. Kimball, et al., "Hysteresis and Delta Modulation Control of Converters Using Sensorless Current Mode," *IEEE Transactions on Power Electronics*, vol. 21, no. 4, pp. 1154 -1158, Jul. 2006.

[19] P. Mattavelli, L. Rossetto, and G. Spiazzi, Small-signal analysis of DC-DC converters with sliding mode control," *IEEE Transactions on Power Electronics*, vol. 12, no. 1, pp. 96-102, Jan. 1997.

[20] V. I. Utkin, "Sliding mode control design principles and applications to electric drives," *IEEE Trans. Ind. Electronics*, vol. 40, no. 1, pp. 23-36, Feb. 1993.

[21] S. C. Tan, Y. M. Lai, and C. K. Tse, "General Design Issues of Sliding-Mode Controllers in DC-DC Converters," *IEEE Transactions on Industrial Electronics*, vol. 55, no. 3, pp. 1160-1173, Mar. 2008.

[22] V. I. Utkin, J. Guldner, and J. X. Shi, *Sliding Mode Control in Electromechanical Systems*. London, UK: Taylor & Francis, 2008.

[23] S. C. Tan, Y. M. Lai, and C. K. Tse, "A Unified Approach to the Design of PWM -Based Sliding-Mode Voltage Controllers for Basic DC-DC Converters in Continuous Conduction Mode," *IEEE Transactions on Circuits and Systems*, vol. 53, no. 8, pp. 1816 -1827, Aug. 2006.

[24] B. S. Yuri, et al., "Boost and Buck-boost Power Converters Control Via Sliding Modes Using Dynamic Sliding Manifold," *in Proc. of the 41st IEEE Conference on Decision and Control*, vol. 3, pp. 2456-2461, Dec. 2002.

[25] S. Baev and Y. Sheessel, "Causal Output Tracking in Nonminimum Phase Boost DC/DC Converter Using Sliding Mode Techniques," *in Proc. of American Control Conference*, pp. 77-82 , Jun. 2009.

[26] Y. He and F. L. Luo, "Study of Sliding Mode Control for DC-DC Converters," *in Proc. of Power System Technology-POWERCON*, pp. 1969-1974, Nov. 2004.

[27] E. Alarcon, et al., "Sliding-mode control analog integrated circuit for switching DC-DC power converter," *in Proc. IEEE International Symposium Circuits and Systems*, vol. 1, pp. 500-503, May. 2001.

[28] A. Visioli, *Practical PID Control*. London, UK: Springer, 2006.

[29] Ramirez, A. and E. Perez, "Stability of Current-mode Control of DC-DC Power Converters," *System and Control Letters*, vol. 45, pp. 113-119, May. 2002.

[30] K. Al-Hosani, A. Malinin, and V. I. Utkin, "Sliding Mode PID Control of Buck Converters," *in Proc. European Control Conference 2009-ECC'09*, Aug. 2009.

[31] H. Sira-Ramirez, "On the Generalized PI Sliding Mode Control of DC-to-DC Power Converters: a Tutorial," *International Journal of Control*, vol. 76, no. 9/10, pp. 1018-1033, Sept./Oct. 2003.

[32] S. C. Tan, Y. M. Lai, and C. K. Tse, "Indirect Sliding Mode Control of Power Converters Via Double Integral Sliding Surface," *IEEE Transactions on Power Electronics*, vol. 23, no. 2, pp. 600-611, Mar. 2008.

[33] Z. S. Chen, W. Z. Gao, J. G. Hu and X. Ye, " Closed-Loop Analysis and Cascade Control of a Nonminimum Phase Boost Converter," *IEEE Transactions on Power Electronics*, April 2011. **26**(4): p. 1237-1252

[34] H. K. Knalil, Nonlinear Systems. Upper Saddle River, NJ: Pearson Prentice Hall, 2002.